Introduction

Plants can be classified into two groups depending on the mechanisms of Fe uptake: Strategy I species, which include dicotyledonous and non-*Graminaceae* monocotyledonous species, and Strategy II plants, which include *Graminaceae* species. Strategy I plants develop a series of root biochemical and morphological changes leading to an increased capacity for Fe uptake when Fe-deprived (see [1], for a review); these responses are accompanied by metabolic changes [2-4]. Morphological changes include root tip swelling, development of transfer cells and an increase in the number of lateral roots [5, 6]. These changes allow for an increase in the root surface in contact with the medium, as a strategy for maximization of Fe uptake [5, 6]. Among the root biochemical changes, there is an induction of a two-step, Fe-uptake system, that consists in a plasma membrane ferric reductase that reduces extracellular Fe(III) to Fe(II) [1, 7-9] and a plasma membrane transporter that imports Fe(II) to the cell [10, 11]. Biochemical responses also include a higher root H^+ extrusion activity, associated to an induction of a plasma membrane H^+-ATPase in rhizodermal cells [12, 13], that enhances Fe solubility. Some Strategy I plants also accumulate and/or release both reducing and chelating substances, including phenolics and flavins, which may have a role in Fe acquisition [14, 15]. Most of these changes are localized in the root tips [4].

At the metabolic level, increases in the activity of PEPC [2, 4], as well as those of several enzymes of the glycolytic pathway (pyruvate kinase, phosphofructokinase, fructose 1,6-bisphosphate aldolase and glyceraldehyde 3-phosphate dehydrogenase (G3PD), [2, 3]) and the TCA cycle (aconitase, fumarase, malate dehydrogenase (MDH) and citrate synthase [2, 4, 16]) have been found in different plant species grown under Fe deficiency. Also, Fe deficiency induces an accumulation of organic acids, mainly malate and citrate, in roots and leaves [17]. The induction of C metabolism (PEPC, glycolysis and TCA cycle) in roots of Fe-deficient plants would provide roots with a source of i) reducing power, protons and ATP for the Fe(III) reductase and H^+-ATPase enzymes, and ii) C from external bicarbonate fixed by PEPC [18]. Carbon could then be exported from the root *via* xylem and used for basic maintenance processes in leaves, which have drastically reduced photosynthetic rates [19]. Iron-deficient plants reorganize its metabolism when resupplied with Fe by changing the morphology of the roots and readjusting the metabolic pathways to the new conditions [20].

The knowledge on the changes with Fe deficiency and resupply of the proteomic and metabolomic profile of roots is still quite scarce. The aim of this work was to characterize these profiles and the changes induced in the root proteome and metabolome in response to Fe deficiency and resupply. This type of studies would provide a holistic view of the metabolic processes occurring in plants under different Fe status.

Materials and Methods

Plant Material

Sugar beet (*Beta vulgaris* L. Orbis from Struße, Dieckmann, Germany) was grown as described elsewhere [20]. Five different types of root tip samples were collected as described in [20]: Fe-sufficient (+Fe), Fe-deficient (-Fe), 24 h Fe-resupplied plants (24h), white root zone of Fe-resupplied plants after 72 h (72h WZ), and yellow zone of Fe-resupplied plants after 72 h (72h YZ).

Protein extraction and analysis

Protein extracts were obtained as described elsewhere [21]. A first dimension, isoelectric focusing (IEF) separation was carried out on ReadyStrip IPG Strips (BioRad), with a linear pI gradient 5-8. Strips were loaded in a PROTEAN IEF Cell (BioRad) and focused at 20 ºC, for a total of 14000 V.h. For the second dimension, polyacrylamide gel electrophoresis (SDS-PAGE), IPG strips were placed onto 12% SDS-PAGE gels to separate proteins between 10 and 100 kDa. Proteins were stained with Coomassie-blue and results analyzed with the PDQuest 8.0 software (BioRad). Two-D gels were made from independent root tip preparations from 3 batches of plants. Protein spots were excised manually and then digested automatically using a Proteineer DP station (Bruker-Daltonics, Bremen, Germany) as described elsewhere [22]. Spectra acquisition was done as described in [23]. Peptide mass fingerprint spectra were measured on a Bruker Ultraflex MALDI TOF-TOF mass spectrometer (Bruker-Daltonics) [23] in positive ion reflector mode. The measured tryptic peptide masses were searched in the NCBInr database, using Mascot software (Matrix Science, London, UK). When available, MS-MS data from LIFT TOF-TOF spectra were combined with MS peptide mass fingerprint data for database searching.

Metabolite extraction, analysis, data processing and statistical analysis

Metabolite extraction (using frozen root tips, ca. 50 mg FW) and analysis followed the recommendations made by the Metabolomics Standards Initiative [24, 25]. After sample extraction and derivatization, samples were analyzed randomly by GC in an Agilent 6890 system connected to a Leco Pegasus IV TOFMS apparatus controlled with Leco ChromaTOF software v.2.32 (Leco, St. Joseph, MI, USA). Data were recorded for 1200 s. GC-TOFMS chromatograms were processed as described by Fiehn et al. [25]. Statistical analysis was performed using univariate, breakdown one-way ANOVA, and multivariate, supervised partial least square (PLS) (with Statistica v. 8.0, StatSoft, Inc.).

Results

IEF-PAGE electrophoresis

The number of polypeptides detected in 2-D gels of root tip extracts from Fe-sufficient and Fe-deficient plans was 141 and 148, respectively (Figs. 1A and 1 B). Averaged 2-D polypeptide maps of root tip extracts from Fe-sufficient and Fe-deficient plants were made from three independent preparations, each from a different batch of plants. To better describe the changes in polypeptide composition, we built a composite averaged virtual map containing all spots present in both Fe-deficient and control root tip extracts (Figs. 1C and 1D). The comparison of averaged maps indicated that Fe deficiency caused increases and decreases in signal intensity in 29 (orange spots in Fig. 1D) and 13 spots (blue spots in Fig. 1C), respectively. Furthermore, 6 and 13 spots were only detected in Fe-sufficient (green spots in Fig. 1C) and Fe-deficient plants (red spots in Fig. 1D), respectively.

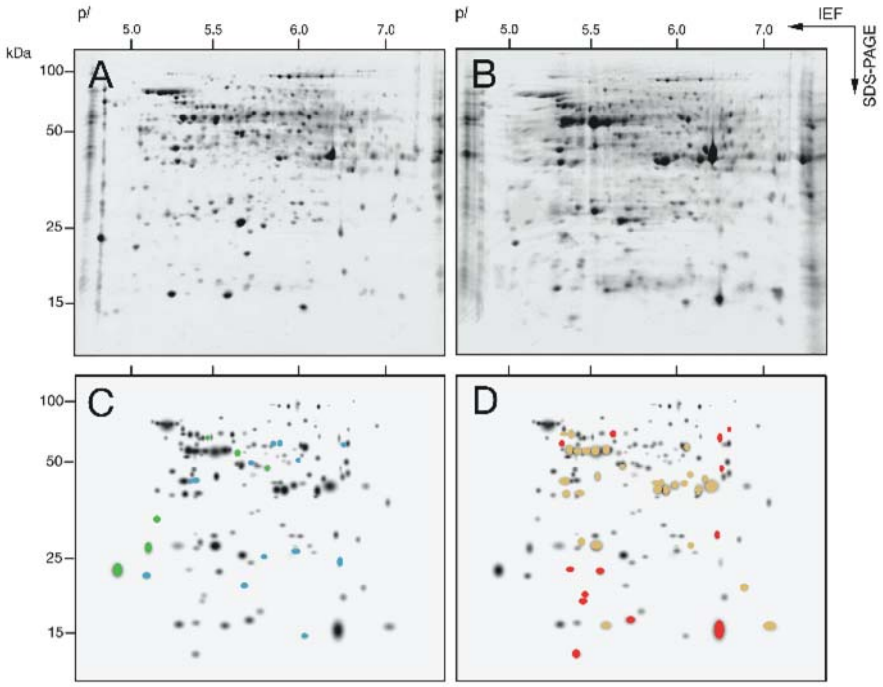

Figure 1. 2-D IEF-SDS PAGE root tip proteome maps from Fe-sufficient and Fe-deficient B. vulgaris plants. Scans of real typical gels of root tips from Fe-sufficient and Fe-deficient plants are shown in A and B, respectively. To facilitate visualization of the spots studied, a virtual composite image (C and D) was created containing all spots present in gels A and B. Spots whose intensities decrease or disappear completely with Fe deficiency were labeled with blue and green spots, respectively (C), and those increasing with Fe deficiency or only present in Fe-deficient gels were labeled with orange and red spots, respectively (D).

From the 29 spots that increased in signal in root tip extracts of Fe-deficient as compared to Fe-sufficient controls, 20 were excised and analyzed by MALDI-MS. Since the sugar beet genome has not been sequenced yet and few sequences are available in the databases, identification was performed by homology searches with proteins from other plant species (not shown). Fourteen proteins from *B. vulgaris* and other species were identified, including proteins related to glycolysis such as fructose 1, 6-bisphosphate aldolase, triose-phosphate isomerase, 3-phosphoglycerate kinase and enolase. Three spots gave significant matches to MDH, and two more polypeptides presented homology with α and ß subunits from F1 ATP synthase. Other proteins that were found to increase in root tip extracts from Fe-deficient sugar beet plants compared to the controls were fructokinase and formate dehydrogenase. Also, one spot gave significant matches to a cytosolic peptidase, At1g79210/YUP8H12R_1. Another spot gave significant match to a glycine rich protein that may have a role in RNA transcription or processing in stress conditions.

From the 13 new spots detected *de novo* in proteome maps from root tip extracts of Fe-deficient plants (Fig. 1D), the 6 more abundant were analyzed by MALDI-MS, resulting in only 2 positive matches. Significant matches were found for G3PD and 6,7-dimethyl-8-ribityllumazine synthase (DMRL) from *S. oleracea.*

From the 13 spots showing a decrease in signal intensity in root tip extracts from Fe-deficient plants when compared to controls (Fig. 1C), 3 were identified by MALDI-MS as a

nucleoside diphosphate kinase, an oxalate oxidase-like germin and the At4g27270 protein from *A. thaliana*, which has oxidoreductase activity and interacts selectively with FMN.

From the 6 spots not detected in root tip extracts from Fe-deficient plants as compared to the controls (Fig. 1C), 3 were identified by MALDI-MS as an oxalate oxidase-like germin, a peroxidase and a caffeoyl CoA O-metyltransferase.

Twelve spots did not change in intensity when the Fe-deficient proteome was compared to the Fe-sufficient one (Fig. 1B), and 7 of them gave significant matches to already known proteins, including 3-phosphoglycerate kinase, glutamine synthetase, and an ascorbate peroxidase. Three more spots gave significant matches with different peptidases, a mitochondrial processing peptidase ß subunit, and α subunit from multicatalytic endopeptidase complex and a ε chain from proteasome. Another spot presented homology to the elongation factor 2 from *B. vulgaris*.

DMRL synthase protein amount analysis

To further analyze the changes induced by Fe status in the amount of DMRL synthase, root tip extracts from sugar beet plants grown in Fe-sufficient, Fe-deficient and Fe-resupplied condition were separated by 2-D IEF-SDS PAGE electrophoresis and gels were analyzed. Real scans of the 2-D gel zone where DMRL synthase protein is located (at 16 kDa, pI 6.6) are shown in Fig. 2. As previously shown in Fig. 1, the DMRL synthase protein was detected *de novo* in Fe-deficient root tip extracts (-Fe, Fig. 2). The spot corresponding to DMRL synthase was also detected in extracts of 24 h and 72 h YZ root samples but not in 72 WZ samples (Fig. 2).

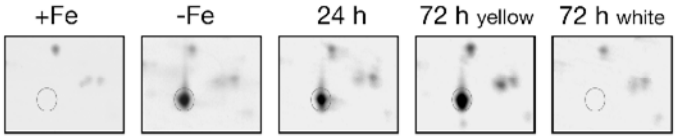

Figure 2. Zoom scans of root tip gels from Fe-sufficient (+Fe), Fe-deficient (-Fe) and 24 h, 72 h YZ and 72 h WZ Fe-resupplied plants.

Metabolite Analyses

Changes induced by Fe deficiency and Fe resupply in whole root tip metabolism where evaluated by non-biased GC-MS metabolite profiling. Partial least squares of the different classes showed a good separation between +Fe and –Fe root tips (Fig. 3). Samples from 72 h WZ were close to +Fe root samples, whereas 24 h and 72 h YZ root samples were more correlated with the –Fe samples. This indicates a reorganization of the root plant metabolism after Fe resupply. A total of 326 metabolites were present in at least 80% of the samples of at least one class. Seventy-six out of the 326 metabolites were identified. Metabolites of the different classes were normalized using the control class (+Fe) values (data not shown). Most metabolites showed a treatment to control ratio higher than 1, indicating a general activation of root tip metabolism with Fe deficiency. The main differences were found among organic acids and sugars. Aminoacids and N compounds did not show large changes, with the exception of nicotianamine, that increased approximately 10-fold in Fe-deficient conditions. Organic acids involved in the TCA cycle increased their concentrations in –Fe conditions, with citrate increasing 21-fold. Oxalic acid decreased 10-fold in –Fe conditions. Among the sugars, there was a remarkable and coordinated increase in the concentration of the raffinose series of oligosaccharides (RSOs), including galactinol, raffinose, lactobionic acid and myo-inositol, which peaked at 24 h after Fe resupply.

Another 46 non-identified metabolites showed significant changes in –Fe and Fe-resupplied plants when compared with +Fe plants.

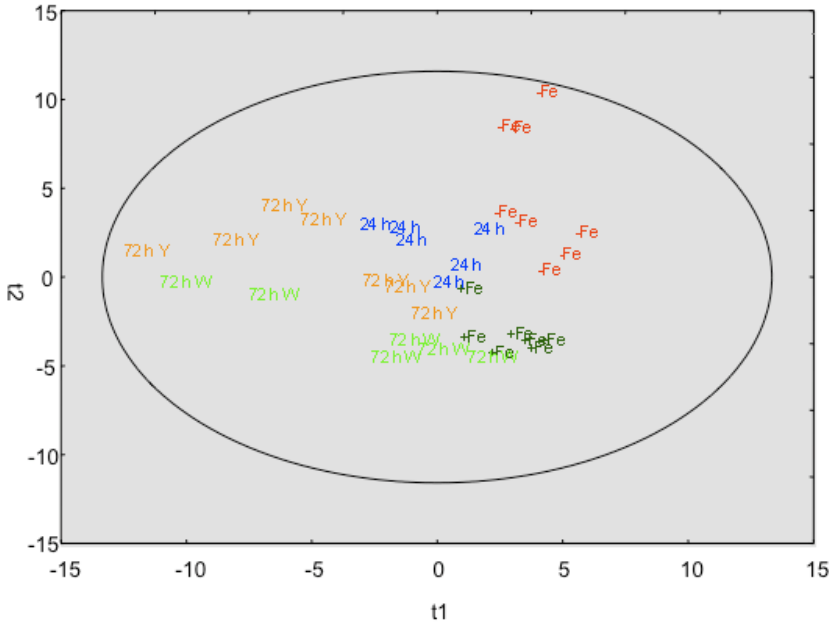

Figure 3. Score scatter plot of component 1 vs. component 2 after Partial Least Square analysis of identified metabolites. Iron-sufficient (+Fe), Fe-deficient (-Fe), 24 Fe-resupplied (24h) and 72 h Fe-resupplied root tip YZ (72 h yellow root zone) and new WZ (72 h white root zone).

Discussion

Most of the proteins found to be up-regulated by Fe deficiency in sugar beet root tips were identified by MALDI-MS as carbohydrate catabolism enzymes. Increases in the activities of glycolysis enzymes in root extracts with Fe deficiency have been previously found, including fructose 1,6-bisphosphate aldolase [26] and G3PD [3, 26, 27]. Also, increases with Fe deficiency in the activities of enzymes such as MDH [2, 4] and those of the TCA cycle have been previously reported. Results are also in agreement with microarray gene analysis of Fe-deficient *A. thaliana* roots [28]. However, increased levels of proteins with Fe deficiency have not been reported so far, with the only exception of G3PD [29]. Up-regulation of carbohydrate catabolism in roots of plants grown in Fe-deficient conditions is probably a result of an increased demand of energy and reducing power in roots, needed to sustain the increased activity of H^+-ATPase and Fe(III)-reductase [1, 28]. Also, two different subunits of F1 ATP synthase increased in Fe-deficient root tips, further supporting the higher energy requirement in these roots. Our results show an increase with Fe deficiency in the amount of formate dehydrogenase, an enzyme related to anaerobic respiration, an alternative pathway for energy production when oxidative phosphorylation is impaired, confirming previous reports based on enzyme activities [4] and transcriptional up-regulation [28].

The largest change found with Fe deficiency in the proteome of root tips corresponds to DMRL synthase, which was detected *de novo* in Fe-deficient root tips, and is the protein with the highest concentration in these gels. DMRL synthase belongs to the five-step riboflavin biosynthesis pathway, and catalyses the last step in the biosynthesis of riboflavin, the precursor

of riboflavin sulphates, FMN and FAD. Riboflavin, riboflavin sulphates and DMRL synthase did not show changes in intensity with Fe-resupply in the root tip yellow parts (not shown). However, *DMRL* gene expression decreased drastically 24 h after Fe resupply (not shown), suggesting that the turnover of this protein is slow. Accumulation in Fe-deficient roots of flavin compounds, including riboflavin and riboflavin 3'- and 5'-sulfate is a characteristic response of sugar beet plants and other species [15, 30-32]. It has been hypothesized, based on the similar location of flavin accumulation and Fe reduction and on the fact that the Fe-reductase is a flavin-containing protein, that flavin accumulation may be an integral part of the Fe-reducing system in roots from Strategy I plants [4]

Plants under Fe deficiency showed an altered carbohydrate metabolism, with an activation of the TCA cycle, including 20-fold citric acid increases. The increases in TCA cycle organic acids with Fe deficiency [4] are coupled with increases in the glycolysis [4] and root C fixation by PEPC [33]. This provides an anaplerotic, non-autotrophic (*via* xylem) [18] C source for leaves which have otherwise reduced photosysnthetic rates. A major change in carbohydrate metabolism was the increase in RSOs compounds that occurs with Fe deficiency and is even boosted in short term Fe resupply. This increase was associated with large decreases in sucrose (RSOs are synthesized from sucrose). RSOs have diverse roles in plants, including transport and storage of C and acting as compatible solutes for protection in abiotic stresses [34, 35]. This is the first report on the activation of RSOs synthesis in plants under Fe deficiency. Regarding N and aminoacid compounds, the only increase was found for nicotianamine, which is thought to play a role in cytosolic Fe trafficking [36, 37].

Literature Cited

1. Schmidt, W., *Mechanisms and regulation of reduction-based iron uptake in plants.* New Phytologist, 1999. **141**: p. 1-26.
2. Rabotti, G., P. De Nisi, and G. Zocchi, *Metabolic implications in the biochemical responses to iron deficiency in cucumber (Cucumis sativus L.) roots.* Plant Physiology, 1995. **107**: p. 1195-1199.
3. Espen, L., et al., *2000 Metabolic responses in cucumber (Cucumis sativus L.) roots under Fe-deficiency: a ^{31}P-nuclear magnetic resonance in-vivo study.* Planta, 2000. **210**: p. 985-992.
4. Lopez-Millan, A., et al., *Responses of sugar beet roots to iron deficiency. Changes in carbon assimilation and oxygen use.* Plant Physiology, 2000. **124**(2): p. 885-897.
5. Kramer, D., et al., *Induction of transfer-cell formation by iron deficiency in the root epidermis of Helianthus annuus L.* Planta, 1980. **147**: p. 335-339.
6. Landsberg, E., *Transfer cell formation in the root epidermis: A prerequisite for Fe-efficiency?* Journal of Plant Nutrition, 1982. **5**: p. 415-432.
7. Moog, P. and W. Brüggemann, *Iron reductase systems on the plant plasma membrane- A review.* Plant and Soil, 1994. **165**(241-260).
8. Susin, S., et al., *The pH requirement for in vivo activity of the iron deficiency-induced "Turbo" ferric chelate reductase - A comparison of the iron-deficiency-induced iron reductase activities of intact plants and isolated plasma membrane fractions in sugar beet.* Plant Physiology, 1996. **110**: p. 111-123.
9. Robinson, N., et al., *A ferric-chelate reductase for iron uptake from soils.* Nature, 1999. **397**: p. 694-697.

10. Eide, D., et al., *A novel iron-regulated metal transporter from plants identified by functional expression in yeast.* Proceedings of the National Academy of Sciences USA, 1996. **93**: p. 5624-5628.
11. Fox, T. and M. Guerinot, *Molecular biology of cation transport in plants.* Annual Review Plant Physiology Plant Molecular Biology, 1998. **49**: p. 669-676.
12. Schmidt, W., *Iron solutions: acquisition strategies and signaling pathways in plants.* Trends in Plant Science, 2003. **8**: p. 188-193.
13. Santi, S., et al. *Water soluble humic substances and Fe-deficiency induce three AHA genes in Arabidopsis*. in *XII International symposium on iron nutrition and interactions in plants*. 2004. Tokio, Japan.
14. Welkie, G. and G. Miller, *Iron nutrition of Nicotiana tabaccum L. in relation to riboflavin, riboflavin-5'-phosphate, and flavin adenine dinucleotide content.* Plant Physiology, 1960. **35**: p. 516-520.
15. Susin, S., et al., *Flavin excretionn from roots of iron-deficent sugar beet (Beta vulgaris L.).* Planta, 1994. **193**: p. 514-519.
16. Landsberg, E., *Function of rhizodermal transfer cells in the Fe stress response mechanisms of Capsicum annuum L.* Plant Physiology, 1986. **82**: p. 511-517.
17. Abadia, J., et al., *Organic acids and Fe deficiency: a review.* Plant and Soil, 2002. **241**: p. 75-86.
18. Lopez-Millan, A., et al., *Effects of iron deficiency on the composition of the leaf apoplastic fluid and xylem sap in sugar beet. Implications for iron and carbon transport.* Plant Physiology, 2000. **124**: p. 873-884.
19. Terry, N., *Limiting factors in photosynthesis. I. Use of iron stress to control photochemical capacity in vivo.* Plant Physiology, 1980. **65**: p. 114-120.
20. Lopez-Millan, A., et al., *Iron resupply-mediated deactivation of Fe-deficiency stress responses in roots of sugar beet.* Australian Journal of Plant Physiology, 2001. **28**: p. 171-180.
21. Meyer, I., et al., *Preparation by two-dimensional electrophoresis of proteins for antibody production: antibody against proteins whose synthesis is reduced by auxin in tobacco mesophyll protoplasts.* Electrophoresis, 1988. **9**: p. 704-712.
22. Shevchenko, A., et al., *Mass Spectrometric Sequencing of Proteins from Silver-Stained Polyacrylamide Gels.* Anal. Chem., 1996. **68**: p. 850-858.
23. Suckau, D., et al., *A novel MALDI LIFT-TOF/TOF mass spectrometer for proteomics.* Analytical and Bioanalytical Chemistry, 2003. **376**: p. 952-965.
24. Sumner, L.W., et al., *Proposed minimum reporting standards for chemical analysis.* Metabolomics, 2007. **3**: p. 211-221.
25. Fiehn, O., et al., *Quality control for plant metabolomics: reporting MSI-compliant studies.* The Plant Journal, 2008. **53**: p. 691-704.
26. Sijmons, P. and H. Bienfait, *Source of electrons for extracellular Fe(III) reduction in iron-deficient bean roots.* Physiologia Plantarum, 1983. **59**: p. 409-415.
27. Rabotti G, D.N.P.a.Z.G., *Metabolic implications in the biochemical responses to iron deficiency in cucumber (Cucumis sativus L.) roots.* Plant Physiology, 1995. **107**: p. 1195-1199.
28. Thimm, O., et al., *Response of Arabidopsis to iron deficiency stress as revealed by microarray analysis.* Plant Physiology, 2001. **127**: p. 1030-1043.

29. Herbik, A., et al., *Iron and copper nutrition-dependent changes in protein expression in a tomato wild type and the nicotianamine-free mutant chloronerva.* Plant Physiol, 1996. **111**: p. 533-40.
30. Welkie, G. and G. Miller, *Iron nutrition of Nicotiana tabaccum L. in relation to riboflavin, riboflavin-5'-phosphate, and flavin adenine dinucleotide content.* Plant Physiology, 1988. **35**: p. 516-520.
31. Welkie, G. and G. Miller, *Iron stress and salt stress responses of lettuce (Lactuca sativa L.).* Journal Plant Nutrition, 1992. **15**: p. 1757-1764.
32. Susin, S., et al., *Riboflavin 3'-Sulfate and 5'-Sulfate, 2 novel flavins accumulating in the roots of iron deficient sugar beet (Beta vulgaris L.).* Journal of Biological Chemistry, 1993. **268**(28): p. 20958-20965.
33. Zocchi, G., et al., *Iron deficiency differently affects metabolic responses in soybean roots.* J Exp Bot, 2007. **58**: p. 993-1000.
34. Bachmann, M., P. Matile, and F. Keller, *Metabolism of the Raffinose Family Oligosaccharides in Leaves of Ajuga reptans L. (Cold Acclimation, Translocation, and Sink to Source Transition: Discovery of Chain Elongation Enzyme).* Plant Physiology, 1994. **105**: p. 1335-1345.
35. Taji, T., et al., *Important roles of drought- and cold-inducible genes for galactinol synthase in stress tolerance in Arabidopsis thaliana.* Plant J, 2002. **29**: p. 417-26.
36. von Wiren, N., et al., *Nicotianamine chelates both FeIII and FeII. Implications for metal transport in plants* Plant Physiol, 1999. **119**: p. 1107-14.
37. Rellan-Alvarez, R., J. Abadia, and A. Alvarez-Fernandez, *Formation of metal-nicotianamine complexes as affected by pH, ligand exchange with citrate and metal exchange. A study by electrospray ionization time-of-flight mass spectrometry*, in *Rapid Communications in Mass Spectrometry*. 2008. p. 1553-1562.